ChemComm

COMMUNICATION

View Article Online
View Journal | View Issue

Check for updates

Cite this: *Chem. Commun.*, 2025, **61**, 2528

Received 29th November 2024,
Accepted 4th January 2025

DOI: 10.1039/d4cc06334a

rsc.li/chemcomm

The synthesis and structural aspects of the perbromo-functionalised thiaboranes *closo*-SB_nBr_n (n = 5, 9, 11): the solid-state structure of the octahedral *closo*-SB_5Br_5, governed by strong dihalogen contacts†

Willi Keller,*[a] Joachim Ballmann,[b] Jindřich Fanfrlík[c] and Drahomír Hnyk*[d]

Co-pyrolysis reactions of B_2Br_4 with S_2Br_2 at 350 °C *in vacuo* yielded the brominated thiaboranes *closo*-SB_5Br_5 (1), *closo*-1-SB_9Br_9 (2) and *closo*-$SB_{11}Br_{11}$ (3), confirmed by high-resolution mass spectrometry, experimental and computational ^{11}B NMR spectroscopy. The strong $Br^{\delta+}$(σ-hole)···$Br^{\delta-}$(ring) attraction has been the decisive energy contribution in the crystal of 1.

Small polyhedral borane and heteroborane clusters of octahedral shape have so far been limited to the borate dianions $[B_6X_6]^{2-}$ (X = H, Cl or Br),[1] the carboranes[2] 1,2- or 1,6-$C_2B_4H_6$ and the perhalogenated heteroboranes $P_2B_4X_4$ (X = Cl[3a] or Br[3b]), $As_2B_4X_4$ (X = Cl[3c] or Br[3d]), SB_5Cl_5,[3e] SeB_5Cl_5[3f,g] and TeB_5Cl_5.[3h] In particular, recent studies of the thermal reactions of B_2Cl_4 with Se_2Cl_2 or $TeCl_4$, producing the octahedral SeB_5Cl_5[3f,g] and TeB_5Cl_5[3h] have shown surprising results: chalcogens heavier than sulphur apparently induce stronger perturbations to the corresponding cluster frameworks, as manifested by the long body diagonal in chlorinated octahedral selena- and telluraboranes, which may prevent their accommodation in octahedral moieties. There are two known pnictogenaboranes, $P_2B_4Br_4$ and $As_2B_4Br_4$, but no brominated octahedral chalcogenaborane as yet, which has prompted us to carry out the thiaborane reaction[3e] with S_2Br_2. On that basis, we wish to report the synthesis and characterisation of *closo*-SB_5Br_5 (**1**) and other new brominated thiaboranes.

We have studied the co-pyrolysis reaction of B_2Br_4 with S_2Br_2 at temperatures above 350 °C. In comparison with chlorinated thiaboranes, prepared at 280 °C, this reaction required significantly higher temperatures because the bromo compounds are less volatile than the Cl-synthons.[3e]

The procedure described yielded three new brominated thiaboranes, *closo*-SB_5Br_5 (**1**), *closo*-1-SB_9Br_9 (**2**) and *closo*-$SB_{11}Br_{11}$ (**3**) (Scheme 1), of which we were able to isolate only compound **1** by repeated vacuum-fractionation and crystallisation processes. Compound **1** was obtained in 5% yield based on the idealised eqn (1). The non-separable compounds **2** and **3** (eqn (2) and (3)) were formed in approximately 1% and 3% yields, respectively.

$$11B_2Br_4 + S_2Br_2 \rightarrow 2SB_5Br_5\ (\mathbf{1}) + 12BBr_3 \quad (1)$$

$$19B_2Br_4 + S_2Br_2 \rightarrow 2SB_9Br_9\ (\mathbf{2}) + 20BBr_3 \quad (2)$$

$$23B_2Br_4 + S_2Br_2 \rightarrow 2SB_{11}Br_{11}\ (\mathbf{3}) + 24BBr_3 \quad (3)$$

The new thiaboranes **1–3** are thermally stable under inert atmosphere at least up to their formation in two experiments at 350 °C and 430 °C. In the very high vacuum applied in EI-MS (10^{-5} mbar), **1** starts to sublime already at 25 °C, **2** at 50 °C and **3** at 85 °C. They are soluble in common aprotic solvents such as benzene, chloroform and methylene chloride.

The corresponding reaction of B_2Cl_4 with S_2Cl_2 has resulted in a much higher number of individual chlorinated thiaboranes *closo*-SB_nCl_n (with n = 4, 5, 6, 9, 10, 11, 12) than in the

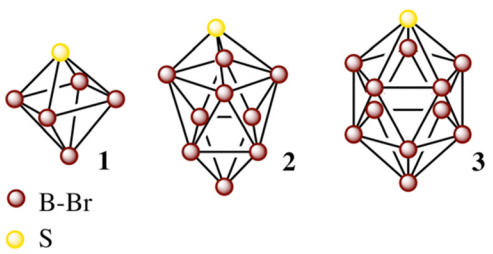

Scheme 1 Molecular diagrams of *closo*-SB_5Br_5 (**1**), *closo*-1-SB_9Br_9 (**2**) and *closo*-$SB_{11}Br_{11}$ (**3**).

[a] *Institut für Chemie, Universität Hohenheim, Garbenstrasse 30, 70599 Stuttgart, Germany. E-mail: willi.keller@uni-hohenheim.de*
[b] *Anorganisch-Chemisches Institut, Ruprecht-Karls-Universität Heidelberg, Im Neuenheimer Feld 270, 69120 Heidelberg, Germany*
[c] *Institute of Organic Chemistry and Biochemistry, Czech Academy of Sciences, Flemingovo nám. 2, 166 10 Praha 6, Czech Republic*
[d] *Institute of Inorganic Chemistry, Czech Academy of Sciences, 250 68 Husinec-Řež, Czech Republic. E-mail: hnyk@iic.cas.cz*

† Electronic supplementary information (ESI) available. CCDC 2403282. For ESI and crystallographic data in CIF or other electronic format see DOI: https://doi.org/10.1039/d4cc06334a

Open Access Article. Published on 06 January 2025. Downloaded on 2/12/2026 6:05:17 PM. This article is licensed under a Creative Commons Attribution-NonCommercial 3.0 Unported Licence.

This journal is © The Royal Society of Chemistry 2025

Open Access Article. Published on 06 January 2025. Downloaded on 2/12/2026 6:05:17 PM. This article is licensed under a Creative Commons Attribution-NonCommercial 3.0 Unported Licence.

present study. This may be attributed to the fact that the isodesmic heats of formation of the bromo-products are less negative than those of the chloro-products.[3e] However, computational studies have confirmed in both cases that octahedral, bicapped square-antiprismatic and icosahedral cages are the most stable in the entire series. The computed isodesmic heats of formation in the origination of *closo*-SB_nBr_n from *closo*-$SB_{n-1}Br_{n-1}$ (n = 5, 9, 11) at the B3LYP/def2-QZVP//BP86/DZVP-DFT level (in kcal mol^{-1}) are as follows:

$$\textit{closo}\text{-1-}SB_4Br_4 + B_2Br_4 \rightarrow \textit{closo}\text{-}SB_5Br_5\ (\mathbf{1}) + BBr_3\ -15.6$$

$$\textit{closo}\text{-4-}SB_8Br_8 + B_2Br_4 \rightarrow \textit{closo}\text{-1-}SB_9Br_9\ (\mathbf{2}) + BBr_3\ -19.6$$

$$\textit{closo}\text{-2-}SB_{10}Br_{10} + B_2Br_4 \rightarrow \textit{closo}\text{-}SB_{11}Br_{11}\ (\mathbf{3}) + BBr_3\ -34.3$$

The new thiaboranes have been characterised by ^{11}B NMR spectroscopy, high- and low-resolution mass spectrometry, X-ray structure determination for **1** and SO-DFT/ZORA/NMR computations (taking spin–orbit coupling (SO) into account), which have confirmed the experimental ^{11}B NMR chemical shifts. With SO not included in ^{11}B NMR chemical-shift computations, the values have shifted upfield by about 5 ppm[4] with respect to the SO-DFT/ZORA/NMR results. Based on these results, we have derived the molecular structures of **1**, **2** and **3** in their solutions (see also Table 1).

The ^{11}B chemical shifts of **1**, **2** and **3** are within the normal range for halogenated heteroborane clusters[3a–h] and closely follow the trends established for non-halogenated heteroboranes.[5a] They also reflect the symmetries of C_{4v}, C_{4v} and C_{5v}, respectively.

As expected, **1** shows two broad signals in a 4 : 1 ratio at −2.3 ppm ($h_{1/2} \approx 106$ Hz, B(2–5)) and 19.4 ppm ($h_{1/2} \approx 113$ Hz, B(6)), which are in agreement with the signals for *closo*-SB_5Cl_5 at −0.3 ppm and 19.4 ppm.[3e] With the application of the Lorentz–Gaussian transformation with a $^1J(^{11}B–^{11}B)$ of 25 Hz, the signals for B(2–5) are split into a quartet, indicating the coupling with B(6) and showing the expected cross-peak in the COSY $^{11}B^{11}B$ NMR with the low-field signal.

The ^{11}B NMR of **2** consists of three signals in a 4 : 4 : 1 ratio at −3.7 ppm (B6–9), 7.5 ppm (B2–6) and 49.6 ppm (B10), which are in good agreement with the signals for *closo*-SB_9Cl_9 at −0.3 ppm, 13.1 ppm and 48.8 ppm.[3e] The signal at −3.7 ppm shows $^{11}B^{11}B$ cross-peak correlation with the other two signals and thus can be assigned to B(6–9), the signal at 7.5 ppm to B(2–5), and the poorly-resolved intensity-one signal at 49.6 ppm can be connected with the antipodal downfield shift[5] of B(10).

The ^{11}B NMR of **3** consists of three signals in a 5 : 5 : 1 ratio at −3.7 ppm (B7–11), −1.4 ppm (B2–6) and 14.2 ppm (B12), with expected cross-peaks between B(7–11)/B(2–6) and B(7–11)/B(12). The signals are in agreement with the chemical shifts established for *closo*-$SB_{11}Cl_{11}$ at −3.9 ppm, 1.0 ppm and 14.4 ppm.[3e]

The 70 eV EI mass spectra of all compounds show a strong molecular ion. In the case of thiaborane **1**, the major cut-off indicates the abstraction of a SBBr edge from SB_5Br_5 to leave a $[B_4Br_4]^+$ fragment. The formation of such a $[B_4Hal_4]^+$ fragment has been analogously found in the mass spectra of *closo*-SB_5Cl_5[3e] and *closo*-1,2-$P_2B_4Cl_4$.[3a] The MS of thiaborane **2** shows the stepwise abstraction of S, Br, BBr_2 and BBr_3 fragments, whereas **3** exhibits only minimal fragmentation with the abstraction of a single Br atom, which indicates the high stability of the icosahedral cluster framework.

All mass-spectroscopy patterns are consistent with the computed spectra based on natural isotopic abundances. On the basis of simple skeletal electron-counting rules,[6] **1**, **2** and **3** should adopt octahedral, bicapped square-antiprismatic and icosahedral geometries, respectively, with sulphur contributing four electrons and each BBr unit two electrons to the cluster bonding. The employment of intrinsic-bond orbitals (IBOs)[3e,g,h] has revealed the nature of bonding in **1**, **2** and **3**. According to the expansion coefficients (ECs: contributions from individual atoms to a particular IBO to reveal the nature of such orbitals), the sulphur involvement in **1** consists of two IBOs with the ECs (the contributing atom in parentheses) of 1.15 (S), 0.51 (B) and 0.25 (B) and one IBO with the ECs of 1.20 (S) and 0.53 (B). Whereas the first pair of IBOs can be assigned to 3c–2e bonding, the second IBO is of 2c–2e type. The rest of the octahedral cage is assembled through 3c–2e IBOs (Fig. 1). The bonding schemes in **2** and **3** are shown in ESI† (Fig. S2).

The ESP (electrostatic potential molecular surface) of **1** is similar to that of its chlorine analogue,[3e] but the bromine

Table 1 The computed[a] and experimental ^{11}B NMR chemical shifts of **1**, **2** and **3**

1 Octahedral motif		
	B(2–5)	B(6)
Comp.	−1.2	20.5
Exp.	*−2.3*	*19.4*

2 Bicapped square-antiprismatic motif			
	B(2–5)	B(6–9)	B(10)
Comp.	8.9	−4.7	53.5
Exp.	*7.5*	*−3.7*	*49.6*

3 Icosahedral motif			
	B(2–6)	B(7–11)	B(12)
Comp.	−1.7	−6.0	14.6
Exp.	*−1.4*	*−3.7*	*14.2*

[a] SOC-PBE0/T2ZP//B3LYP/6-311 + G**.

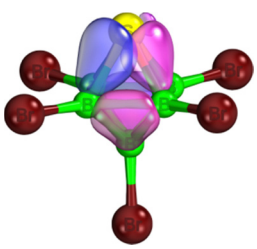

Fig. 1 Visualised IBOs for SB_5Br_5 (**1**). The colour coding is as follows: blue classical 2c–2e bonding, pink 3c–2e bonding.

Open Access Article. Published on 06 January 2025. Downloaded on 2/12/2026 6:05:17 PM.
This article is licensed under a Creative Commons Attribution-NonCommercial 3.0 Unported Licence.

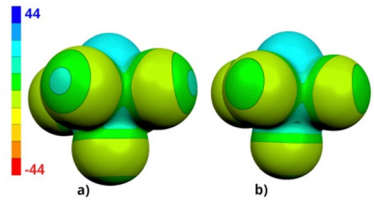

Fig. 2 The ESP molecular surfaces of **1** (a) and SB_5Cl_5 (b) computed at the HF/cc-pVDZ level.

Table 2 The minimum and maximum values of the ESP molecular surfaces computed at the HF/cc-pVDZ level

	$V_{s,max}$ [kcal mol^{-1}]		$V_{s,min}$ [kcal mol^{-1}]
Compound	Sulphur atom	Halogen atoms	Halogen atoms
SB_5Br_5(**1**)	24.5	4 × 11.6; 10.2	4 × −6.0; −5.8
SB_5Cl_5	24.8[3e]	4 × 6.6; 5.7	4 × −5.6; −5.1

atoms of **1** have more positive σ-holes than the chlorines of SB_5Cl_5 (see Fig. 2 and Table 2).

To confirm the octahedral structure of **1**, single crystals were grown *via* vacuum sublimation and subjected to X-ray diffraction (see Fig. 3). Compound **1** crystallises in $P2_1/c$ with three crystallographically independent *closo*-SB_5Br_5 octahedrons present in the corresponding asymmetric unit. As a consequence of symmetry, a total of twelve molecules are present in the centrosymmetric monoclinic cell (see ESI,† for details). Crystal packing is dominated by short contacts between the bromine atoms of neighbouring molecules, indicative of dihalogen bonding (d(Br···Br) = 339 to 368 pm, see also Fig. 4). Intermolecular bonding interactions between the sulphur and the bromine atoms, however, seem to be absent because no short contacts (<the sum of vdW radii) have been observed.

All the interaction motifs present in the crystal structure of **1** have been investigated using a cluster model. Two-body interaction energies have been computed for the selected crystallographic molecule using the SAPT method,[7] which enables

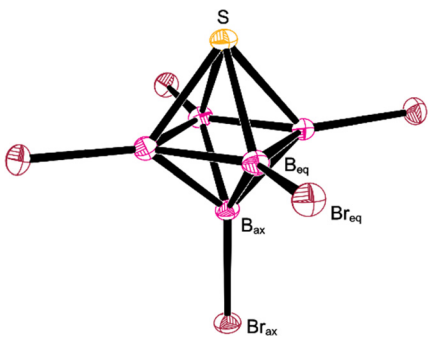

Fig. 3 ORTEP plot (thermal ellipsoids drawn at the 50% probability level) of the molecular structure of *closo*-SB_5Br_5 (**1**). The asymmetric unit contains three independent molecules with very similar metrical parameters; only one of these molecules is shown. Selected averaged bond lengths (pm) and angles (°): B_{eq}–Br_{eq} 189.4(5), B_{ax}–Br_{ax} 190.4(5), S–B_{eq} 196.8(**2**), B_{eq}–B_{eq} 177.8(7), B_{eq}–B_{ax} 170.1(**3**), B_{eq}–S–B_{eq} 53.7(**2**), B_{eq}–B_{eq}–B_{eq} 90.0(**3**), B_{eq}–B_{ax}–B_{eq} 63.0(**3**), S–B_{ax}–Br_{ax} 179.1(**2**).

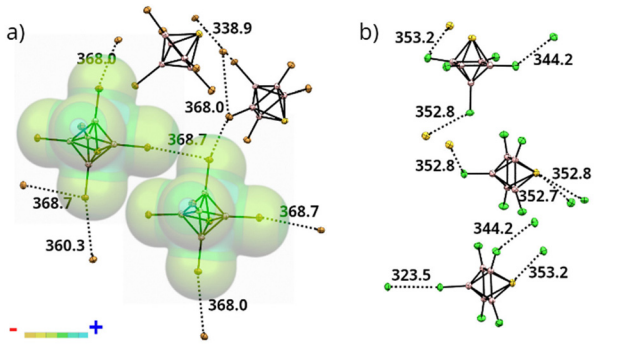

Fig. 4 The short contacts below the sum of vdW radii in the crystal packing of **1** (a) and SB_5Cl_5[3e] (b) are indicated by dot lines (in pm). An example of $Br^{\delta+}\cdots Br^{\delta-}$ is depicted in term of the corresponding molecular ESP surfaces. The color coding of the ESP is in the range of −26 to 26 kcal mol^{-1}.

energy decomposition into individual terms. For comparison, the same analysis has also been performed for SB_5Cl_5. Both crystals are dominated by dispersion as expected. Surprisingly, the contribution of dispersion to crystal packing was slightly less pronounced in **1** than in SB_5Cl_5 (*i.e.* the dispersion in them formed 63 and 67%, respectively, of the sum of all the attractive terms in the SAPT decomposition). The explanation is that there are considerably more positive σ-holes on Br atoms in **1** than on Cl atoms in SB_5Cl_5. Compound **1** thus has a better balance of positive and negative sites for crystal packing – it has six highly positive σ-holes and five negative rings around B–Br bonds, unlike SB_5Cl_5, which has only one highly positive σ-hole on the S atom to match the five negative rings around B–Cl bonds. Consequently, the electrostatic contribution is more pronounced in the crystal packing of 1, which is dominated by dihalogen bonds, than in SB_5Cl_5, dominated by chalcogen bonds (see Fig. 4 and Table 3). This enhanced electrostatic contribution may be ascribed to the fact that the crystallisation process of **1** is more straightforward than that of SB_5Cl_5.

In a thermodynamically controlled reaction at 350 °C, simple inorganic synthons such as B_2Br_4 and S_2Br_2 have provided octahedral, bicapped square-antiprismatic and icosahedral structural motifs referred to as *closo*-SB_5Br_5, *closo*-1-SB_9Br_9 and *closo*-$SB_{11}Br_{11}$, respectively. Structural features have been elucidated through a combination of experimental and computational approaches including NMR spectroscopy together with MS spectrometry and DFT/ZORA/NMR model chemistry. These methods have confirmed that these three structural arrangements are

Table 3 The interaction energies (ΔE^2) computed at the SAPT0/jun-cc-pVDZ level have been decomposed into electrostatic (E_{elec}), exchange (E_{exch}), induction (E_{ind}) and dispersion (E_{disp}) contributions using the SAPT methodology. All the energies are in kcal mol^{-1}. The relative values in round brackets indicate the contribution to the sum of all the attractive terms

Compound	ΣSAPT0	ΣE_{elec}	ΣE_{exch}	ΣE_{ind}	ΣE_{disp}
SB_5Br_5 (**1**)	−41.5	−38.8 (30%)	86.4	−8.7 (7%)	−80.4 (63%)
SB_5Cl_5	−32.2	−24.0 (26%)	59.4	−6.1 (7%)	−61.5 (67%)

This journal is © The Royal Society of Chemistry 2025

Open Access Article. Published on 06 January 2025. Downloaded on 2/12/2026 6:05:17 PM. This article is licensed under a Creative Commons Attribution-NonCommercial 3.0 Unported Licence.

good representations of the molecular geometries in solutions. In addition, crystal-structure determination of the octahedral brominated thiaborane shows that the Br···Br contacts are strong enough to be able to overcome the repulsion between the σ-holes located on the bromines and the sulphur. As a consequence, the crystal-packing forces are dominated by strong $Br^{\delta+}$(σ-hole)···$Br^{\delta-}$(ring) attraction, *i.e.* the crystal is formed without chalcogen bonding detected in the chlorine analogue of **1**.

We thank Dr Jürgen Conrad and Mr Mario Wolf (Institut für Chemie, Universität Hohenheim) for recording NMR spectra and Dipl.-Ing. (FH) J. Trinkner (Institut für Organische Chemie, Universität Stuttgart) for recording MS. Dr M-B. Sárosi (Universität Würzburg) is thanked for the assistance with the ADF computations. Financial support from the Czech Science Foundation, grant no. 23-05083S, is gratefully acknowledged.

Data availability

The data supporting of this article have been included as part of the ESI.† The crystallographic data for compound **1** (*closo*-SB_5Br_5) were deposited with the Cambridge Crystallographic Data Centre with CCDC no. 2403282.†

Conflicts of interest

There are no conflicts to declare.

Notes and references

1 For selected surveys on polyhedral boranes, see: (*a*) W. N. Lipscomb, *Boron Hydrides*, Benjamin, New York, 1963; (*b*) E. L. Muetterties, *Boron Hydride Chemistry*, Academic Press, New York, 1975; (*c*) J. F. Liebman, A. Greenberg and R. E. Williams, *Advances in Boron and the Boranes*, VCH Verlagsgesellschaft, Weinheim New York, 1988; (*d*) R. B. King, *Chem. Rev.*, 2001, **101**, 1119–1152.

2 For selected surveys on carboranes, see: (*a*) *Electron Deficient Boron and Carbon Clusters*, ed. G. A. Olah, K. Wade and R. E. Williams, John Wiley and Sons, New York, 1991; (*b*) T. Onak, Polyhedral Carbaboranes, *Comprehensive Organometallic Chemistry II*, ed. E. W. Abel, F. G. A. Stone and G. Wilkinson, Pergamon, Oxford, UK, 1995, Vol. 1, 217–255; (*c*) M. A. Fox, Polyhedral Carboranes, *Comprehensive Organometallic Chemistry III*, ed. R. H. Crabtree and D. M. P. Mingos, Elsevier, 2007, Vol. 3, 49–112; (*d*) R. N. Grimes, *Carboranes*, ed., Elsevier, Amsterdam, The Netherlands, 2016.

3 (*a*) W. Haubold, W. Keller and G. Sawitzki, *Angew. Chem., Int. Ed. Engl.*, 1988, **27**, 925–926; (*b*) W. Keller, L. G. Sneddon, W. Einholz and A. Gemmler, *Chem. Ber.*, 1992, **125**, 2343–2346; (*c*) R. Schäfer, W. Einholz, W. Keller, G. Eulenberger and W. Haubold, *Chem. Ber.*, 1995, **128**, 735–736; (*d*) W. Keller, W. Einholz, D. Rudolph and T. Schleid, *Z. Anorg. Allg. Chem.*, 2017, **643**, 664–668; (*e*) W. Keller, F. Lissner, J. Ballmann, J. Fanfrlík, D. Hnyk and T. Schleid, *Angew. Chem., Int. Ed.*, 2024, **63**, e202406751; (*f*) W. Keller and M. Hofmann, *Z. Anorg. Allg. Chem.*, 2017, **643**, 729–731; (*g*) W. Keller, M. Hofmann, H. Wadepohl, M. Enders, J. Fanfrlík and D. Hnyk, *Dalton Trans.*, 2023, **52**, 16886–16893; (*h*) W. Keller, J. Ballmann, M. B. Sárosi, J. Fanfrlík and D. Hnyk, *Angew. Chem., Int. Ed.*, 2023, **62**, e202219018.

4 See e.*g.* (*a*) W. Keller, M. Hofmann, M. B. Sárosi, J. Fanfrlík and D. Hnyk, *Inorg. Chem.*, 2022, **61**, 16565–16572; (*b*) W. Keller, M. B. Sárosi, J. Fanfrlík, M. Straka, J. Holub, M. L. McKee and D. Hnyk, *RSC Adv.*, 2023, **13**, 19627–19637.

5 (*a*) S. Heřmánek, *Chem. Rev.*, 1992, **92**, 325–362; (*b*) F. Teixidor, C. Vinas and R. W. Rudolph, *Inorg. Chem.*, 1986, **25**, 3339–3346; (*c*) T. P. Fehlner, P. T. Czech and R. F. Fenske, *Inorg. Chem.*, 1990, **29**, 3103–3109; (*d*) S. Heřmánek, D. Hnyk and Z. Havlas, *J. Chem. Soc., Chem. Commun.*, 1989, **23**, 1859–1861; (*e*) M. Bühl, P. V. R. Schleyer, Z. Havlas, D. Hnyk and S. Heřmánek, *Inorg. Chem.*, 1991, **30**, 3107–3111.

6 (*a*) R. E. Williams, *Inorg. Chem.*, 1971, **10**, 210–214; (*b*) K. Wade, *Adv. Inorg. Chem. Radiochem.*, 1976, **18**, 1–66; (*c*) R. E. Williams, *Adv. Inorg. Chem. Radiochem.*, 1976, **18**, 67; (*d*) R. W. Rudolph, *Acc. Chem. Res.*, 1976, **9**, 446–452; (*e*) R. E. Williams in *Electron Deficient Boron and Carbon Clusters*, ed. G. A. Olah, K. Wade and R. E. Williams, Wiley and Sons, New York, 1991, 11–93; (*f*) R. E. Williams, *Chem. Rev.*, 1992, **92**, 177–207.

7 T. M. Parker, L. A. Burns, R. M. Parrish, A. G. Ryno and C. D. Sherrill, *J. Chem. Phys.*, 2014, **140**, 094106.